A vision based reverse engineering approach to surface digitizing in restorative dentistry

K. Alemzadeh & L. Zhang
Department of Mechanical Engineering, University of Bristol, Bristol, U.K.

Abstract

Computer Aided Design and Manufacture (CAD/CAM), and Reverse Engineering (RE) are employed to machine and enhance the fitting accuracy of ceramic inlays. A vision system (VS) based Reverse Engineering approach is currently being developed for surface digitizing where two dimensional (2-D) images of the teeth from CCD cameras are used to create three dimensional (3-D) CAD model. This approach involves using shape recovery from a series of profile images of teeth. A camera calibration technique is used to minimize the image distortion caused by lenses. Assuming the teeth have no regional concaved surface (e.g. incisors), the slicing algorithm, derived from occluding boundaries technique, attempts to generate surface point data (point cloud) from the profile images. Disparity maps of various teeth between this VS and Renishaw plc.'s dental Triclone system has been carried out to evaluate the accuracy of the VS.
Keywords: vision system, slicing method, surface reconstruction, restorative dentistry.

1 Introduction

Reverse Engineering (RE) is an advanced reverse design technique to create 3-D free form surfaces from an existing physical model using laser or contact probe as a surface digitizer [1]. RE is used as a powerful tool for initial conceptual and aesthetic design, product prototyping, performance testing, and model modification needed for obtaining an optimal product design [2]. A vision system uses an optical scanning method similar to laser probe but it is safer.

The use of vision systems in dentistry predominantly centres on dental restoration [3]. This involves the fabrication of crowns and inlays through to complete mouth restructuring [3, 4]. The UK dental market is worth over £2.5bn of which dental restoration represents over a third [5]. This is likely to grow over the coming years as the public learns about newer, more aesthetic ceramic materials and quicker, cheaper processes [5, 6].

Nowadays, the importance of tooth modelling in dentistry has been exploited. It has been recognized that resistance to restoration failure is not solely a biological concern (e.g. toxicity), but that the cavity shape, dimensions, and the state of stress must all be taken into account [3, 4, 6, 7, 8]. However, current scanning technologies, laser or contact probes both have their own limitations [9, 10] in tooth surface digitizing. Laser scanners are usually expensive and incapable of scanning mirror-like surfaces. Coordinate Measuring Machines (CMM) with contact probes are excellent in measuring accuracy, but often time consuming and unsuitable for soft or flexible objects [1, 2]. Upon this, three-dimensional (3-D) optical digitizers have become a better choice for restorative dentistry application [4, 6]. Mörmann and Brandestini (1989) introduced the first optical based CAD/CAM system - Cerec 1 - for use in computer-aided production of ceramic inlays [11].

The vision system (VS) in the University of Bristol focuses on developing an off-line 3-D modelling of computer controlled production technologies in restorative dentistry. The aim is to improve the quality of the construction units to help patient care and at the same time to lower manufacturing costs by simplifying the method and reducing the production time [5, 7]. This paper is investigating and developing a new vision system in restorative dentistry and its potential for other applications in collaboration with Renishaw.

2 The three-phases approach

The VS integrates three development phases: 1) Vision system rig prototype (VSRP), 2) Vision system techniques (VST), and 3) Vision system software (VSS). The VSRP is for multiple image acquisition in conjunction with the methods used for image processing. The VST, which integrates depth recovery techniques [12] and multiple images processing, involves camera calibration [13, 14], edge detection [15, 16, 17] and surface modeling development (e.g. slicing algorithms) [3, 15, 16, 17, 18]. The VSS finally converts (or uses existing software) VST into programs used to digitize surface point data and reconstruct the surface models which can be used in downstream process, such as CAD Design, Computer Aided Tissue Engineering [19, 20], Finite Element Analysis [3, 21, 22] and Rapid Prototyping [23].

2.1 Phase 1: VSRP development

The complete work flow chart of the VS is shown in Figure 1. A vision system rig was built to acquire required images incorporating with different 3-D depth recovery methods for point data generation. The rig was constructed to be able to accommodate up to *3* CCD cameras for further implementation of the Stereo Vision technique, although only the horizontal camera was used at this stage for Slicing Method. The rig also had a built-in turntable with the ability to turn in *360* degrees holding physical objects (e.g. incisor) for image acquisition. Moreover, environment lighting effect on the image quality was also taken into account; and therefore a set of 9 lights were installed around the rig which would be fully covered by light-tight boards in the image acquisition process.

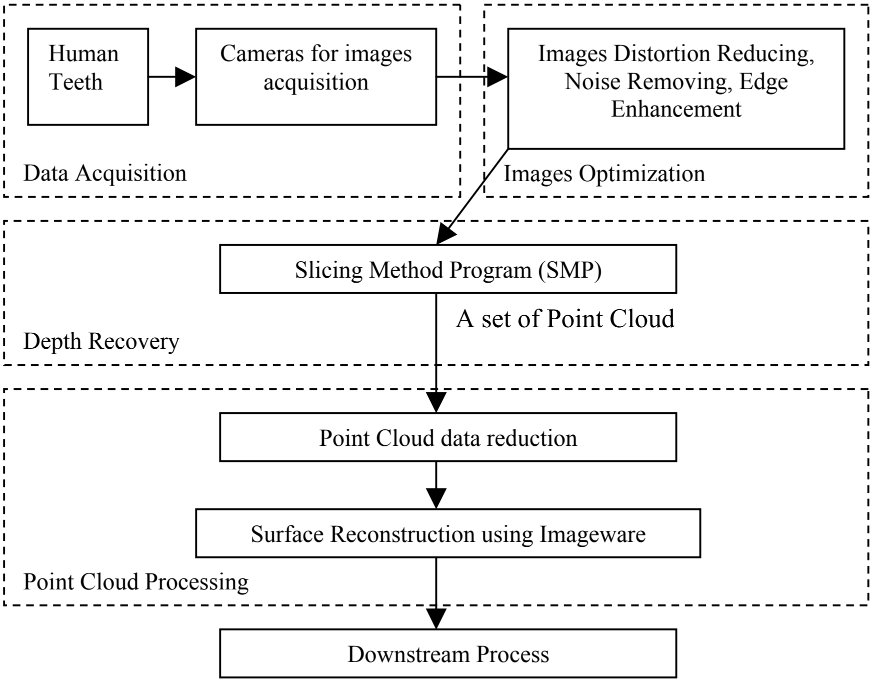

Figure 1: The flow chart of our VS.

2.2 Phase 2: VST development

The field of computer vision that relates to RE is depth recovery. Techniques of converting 2-D images to 3-D point data are called depth recovery, which is a classic problem in computer vision [24]. The point cloud processing deals with the point cloud to surface problem. At this stage surfaces from point clouds are reconstructed using Imageware [25], which is a free-form styling software distributed by UGS.

Occluding Boundaries (OB) technique and its derivative, the Slicing Method, were the main 3-D depth recovery methods used in this project. OB usually consists of one camera and relative motion between object and camera [26]. When the object is rotated in different angles, a number of profile views can be taken and then the objective is to recover shape from these profile view images. For each view, the silhouette (3-D boundary) of the object is extracted using edge detection. These profile views can be used to create a series of occluding boundaries. Each occluding boundary is effectively the rim of the object projected in the image plane. Figure 2 shows the visual perception process of the Slicing Method. With the Slicing Method many profile views of an object are captured from different angles. As per all Occluding Boundaries techniques these images are then binarised (edge detection), so that each image of the object is a silhouette. Each silhouette is then 'sliced' into one pixel high segments, which can then be projected onto a new image. This new image is a cross sectional slice at a specific height of a particular view. Once a complete set of slices exists for each view, a union operation can be performed on corresponding slices from all the views. When all union operations have been completed a final set of slices will have been produced that contains the data for the 3-D model of the object.

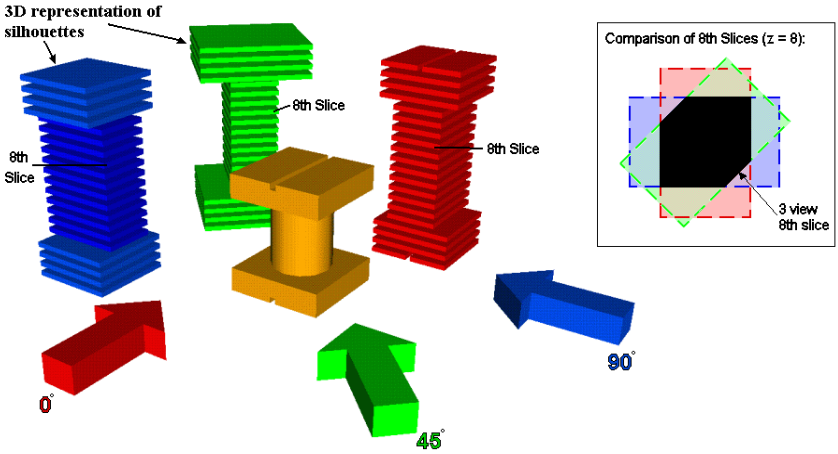

Figure 2: Visual representation of the Slicing Method, the boxed section shows an example union operation with the 8th slice.

2.3 Phase 3: VSS development

2.3.1 Camera Calibration process

The aim of camera calibration in the context of 3-D vision systems is the process of determining the internal camera geometric and optical characteristics (intrinsic parameters) and/or the 3-D position (Translation) and orientation (Rotation) of the camera frame relative to a certain world coordinate system (extrinsic parameters) [13, 14]. In this case, the certain world coordinate system refers to physical objects. The intention of carrying out camera calibration is mainly because of the distortion brought by the lens. It is known that the optical distortion of lens and non-linearity of the CCD camera will influence getting the correct and accurate image [16, 27].

In order to reduce the distortion, telecentric lenses were selected because they eliminate distortion by collimating the light entering the lens [27]. In a telecentric lens configuration, all chief rays are parallel to the optical axis.

2.3.2 3-D objects edge detection

The main technique used here is greyscale *Thresholding*, which is useful to separate out the region of the image corresponding to objects in background [17]. The input to the thresholding operation is a greyscale image and the output is a binary image representing the segmentation. In this study, the segmentation is determined by a single parameter known as the intensity threshold. Usually, black pixels correspond to background and white pixels correspond to foreground (or vice versa) [16]. Let T = threshold intensity, $P(x, y)$ = each pixel intensity. In a single pass, $P(x, y)$ is compared with T, If $P(x, y) \geq T$, pixel is usually set to white; if $P(x, y) < T$, pixel is usually set to black [15, 16]. Using lighting to eliminate the shadow on the objects, which increases the contrast in the image, will largely improve the thresholding accuracy. Edge-detection procedure is carried out by WIT studio, which is a visual graphical programming software for designing computer algorithms (e.g. image processing) [18].

2.3.3 Slicing method program

The Slicing method program (SMP) was also compiled within WIT environment. Figure 3 shows the visual perception of slicing method in processing a tooth preparation model.

By applying SMP to the profile images, object slices are created with the information of every edge point coordinate for each slice. These edge points are the object surface point data for downstream process. In bioengineering such as computer aided tissue engineering [19, 20], usually the slice images generated are interpreted into a volumetric model. However, there are many advantages of converting these images into a CAD based model in bioengineering [19]; this is why the SMP interprets the slice images into point cloud which can be easily converted to CAD model for many downstream processes.

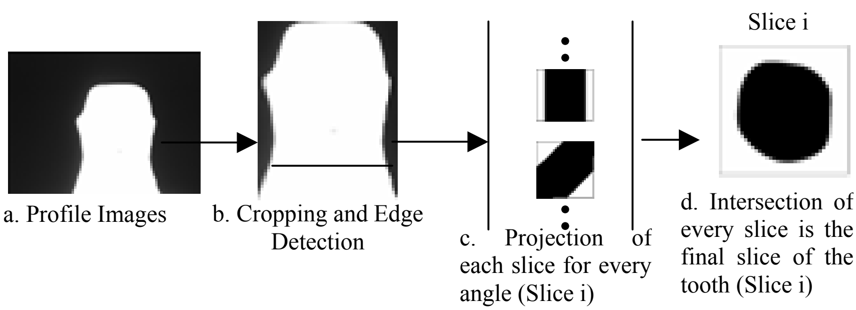

Figure 3: Slicing method in processing a tooth preparation model (example shown on a sample slice i): a) Profile Images, b) Cropping and Edge Detection, c) Projection of each slice for every angle (Slice i), d) Intersection of every slice is the final slice of the tooth (Slice i).

3 Application examples

To evaluate the VS accuracy, the tooth preparation model provided by Renishaw and an additional cracked 7-year-old child incisor by the first author, were digitized by the VS using the SMP. These two samples were also scanned by Renishaw's Triclone dental system with *10* μm accuracy. The Triclone accuracy was compared with the VS. This comparison was demonstrated with the VS point cloud and the surface generated by Triclone point cloud.

3.1 Image acquisition

40 profile images were captured using a SONY XC-ST70 CCD camera with a Computar TEC M55 telecentric lens. The angle increment between each pair of neighbourhood images was 4.5^o. The images captured had a resolution of 640×480. The CCD camera here had effective pixels of 768×494.

3.2 Image correction

Firstly, in order to reduce the distortion caused by the lens, the calibration process described by Jean [13] was used. Secondly, the scale factors in both horizontal and vertical directions of profile images were calculated by carrying out 2D dimension test. Each square has the dimension 5mm × 5 mm. For each square, the pixel numbers were calculated both directions. Then the scale factors = real size dimension /pixel number.

3.3 SMP results

Figure 4 (a) and (b) respectively show the process of the cracked child tooth and the tooth preparation to point data. The cracked child incisor and tooth preparation were divided into *349* and *487* slices respectively by the SMP. The cracked incisor point cloud had *208,631* points and the tooth preparation point cloud had *139,498* points. These point clouds had quite a huge density and should be reduced before surface reconstruction. This huge density was partly caused by the low resolution of the images which made the teeth edges jagged. This error can be overcome by higher resolution cameras and better edge enhancement. The cracked region of the child's tooth was the key area which was given the greatest attention. This area's point cloud accuracy was discussed in the following results evaluation parts. The SMP has the ability to interpret up to *1,000* slice images. For 500 slices, it usually takes around 2 and a half hours to run on the platform of Pentium P4 2.6G HZ and Memory 1Gb.

3.4 Evaluation of the results

These two samples were also scanned by Renishaw's Triclone dental system, which has an accuracy of *10* μm. Figure 5 (a) and (b) show these two Triclone point clouds respectively. In order to obtain a relatively accurate result of the comparison, the Triclone point clouds were surface reconstructed using

Imageware styling software [25]. Figure 5 (c) and (d) show the comparison of this reconstructed surface and the VS point cloud of the cracked child's incisor. Figure 5 (e) shows the same comparison of the tooth preparation. Figure 5 (f) shows the disparity map between the Triclone surface and VS point cloud of the incisor. In the disparity map, the cracked region of the incisor was marked by a rectangle. This area showed a deviation difference less than *100* µm. Figure shows a very accurate comparison result in profile view. The difference between the Triclone surface and VS point cloud is currently not possible to be ascertained accurately due to the coordinate system difference and alignment difficulty.

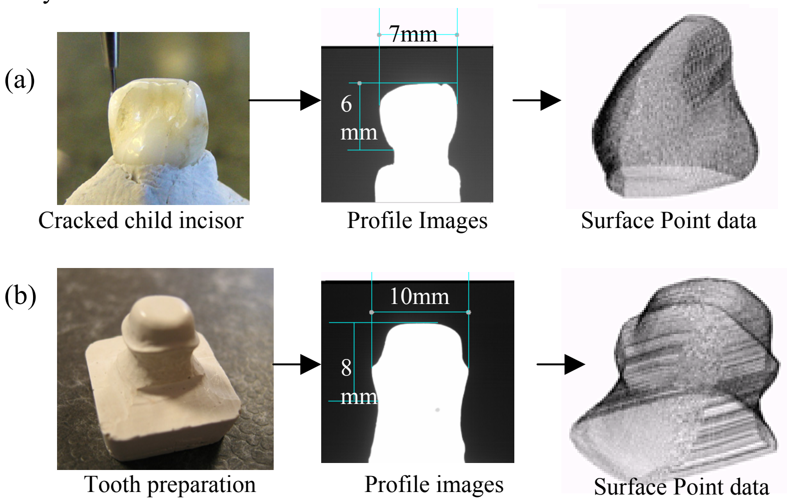

Figure 4: Results of SMP on two samples.

The comparison shown in Figure 5 is through a manual intervention of translation and rotation to superimpose the surface and point cloud. Therefore, the disparity map in Figure 5 (f) can only be recognized for the purpose of demonstration. However, this comparison result has been very promising for restorative dentistry, because the dental Triclone dental system has quite a fine accuracy of *10* µm. And this point cloud to surface alignment problem can be improved by more intelligent registration methods [28].

4 Conclusion and future work

A VSRP has already been designed, fabricated and tested which is capable of scanning different types of objects, especially in the area of restorative dentistry. The VSRP functions have been demonstrated by applying to two typical samples used in dentistry. The point clouds obtained by the VS had a very satisfying density compared to Triclone. SMP has shown its potential in processing a single tooth. Current development concentrates on a final integrated system, incorporating Stereo Vision technique and LED structure lighting devices, in order to make the VS more intelligent and accurate. Furthermore, an automatic surface reconstruction algorithm and environment is under development to fit the B-spline surface on the point cloud obtained by the VS. The developed VS can also be applied to the insect wing motion simulation systems. And this has important industrial, civil and military applications. This Vision System will be used to attempt to digitally capture the insect wing and hinge shape [29], which consists of relatively complex biological structure that conventional CAD design cannot directly model and both CMMs and laser scanners are incapable of digitizing.

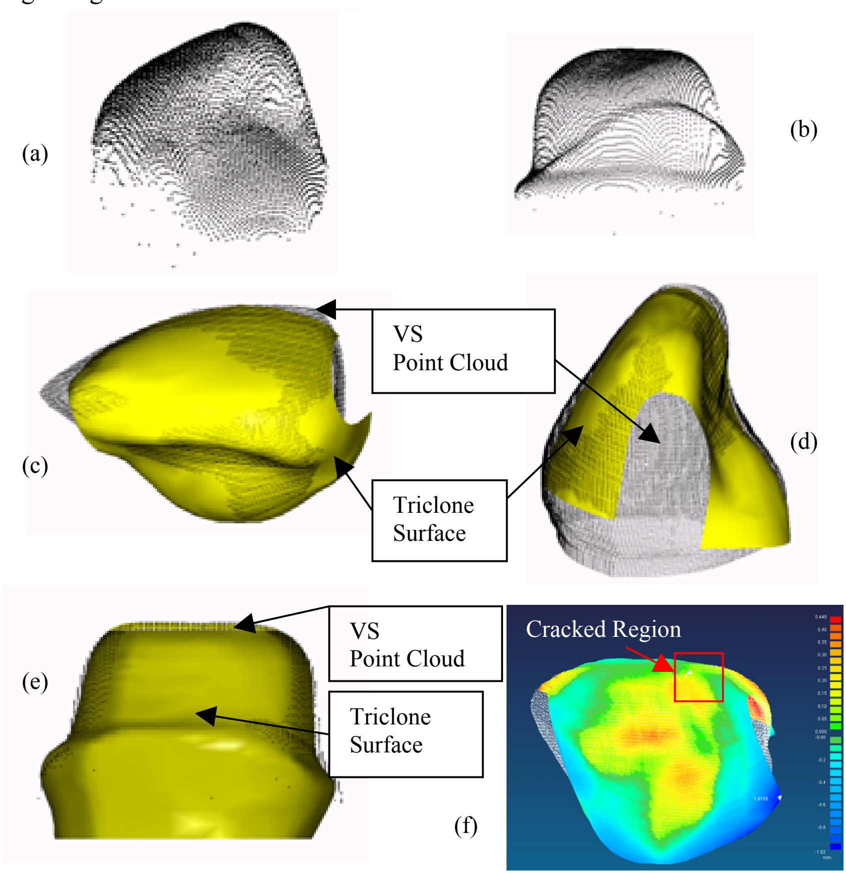

Figure 5: Evaluation of the SMP results: a) Cracked Child Incisor (Triclone, 6,103 points), b) Tooth Preparation (Triclone, 6,984 points), c) Comparison of Triclone surface and VS point cloud (child incisor, top view), d) Comparison of Triclone surface and VS point cloud (child incisor, profile view), e) Comparison of Triclone surface and VS point cloud (tooth preparation, profile view) and, f) Disparity map between the Triclone surface and VS point cloud (incisor, average deviation: 157 µm).

Acknowledgements

We would like to thank Renishaw plc for donating the Cyclone scanning machine, various other dental materials and their constant support throughout the project.

References

[1] Armstrong, P. J. & Antonis, J. (2000).The development of an active computer Vision System for Reverse Engineering. Proceedings of the Institution of Mechanical Engineers, Part B: Journal of Engineering Manufacture: Vol. 214; 615-618.

[2] Aoyama, H. & Suzuki, Y. (2000). Autonomous Measurement of Physical Model Shape for Reverse Engineering. Journal of Manufacturing System: Vol. 19; no.6; 375-381.

[3] Lin, C. L., Chang, C. H. & Ko, C. C. (2001). Multifactorial analysis of an MOD restored child premolar using auto-mesh finite element approach. Journal of Oral Rehabilitation: Vol. 28; 576-585.

[4] Paulus, D., Wolf, M., Meller, S. & Niemann, H. (1999). Three-dimensional computer vision for tooth restoration. Medical Image Analysis; Vol. 3(1); 1–19.

[5] Office of Fair Trading. http://www.oft.gov.uk/default.htm

[6] P Xinmin L., Zhongqin, L. & Ziping, Z. (2001). A study of a Reverse Engineering System Based on Vision Sensor for Free-Form Surfaces. Computers & Industrial Engineering: Vol. 40; 215-227.

[7] Duret, F. (1988). CAD/CAM in dentistry. J. Amer. Dent. Assoc.: Vol. 117; 715-720.

[8] Chen, L. C. (2003). Development of Innovative 3-D Dental Measurement Technique and Manpower for Tooth Model Restoration through University-Industry Collaboration Programmes. International Conference on Engineering Education.

[9] Malamas, E. N., & Petrakis, E.G.M. (2003).A survey on industrial Vision Systems, applications and tools. Image and Vision Computing: Vol. 21; 171-188.

[10] Batchelor, B. & Whelan, P. (2002).Intelligent Vision Systems for Industry.

[11] Schmidseder, J. (2000). Aesthetic Dentistry: Color Atlas of Dental Medicine: Thieme.

[12] Sakarya, U. & Erkmen, I. (2003). An improved method of photometric stereo using local shape from shading. Image and Vision Computing: Vol. 21; 941-954.

[13] Bouguet, J. (2004). Camera Calibration Toolbox for Matlab. http://www.vision.caltech.edu/bouguetj/calib_doc/.

[14] Zhang, Z. Y. (1999). Flexible Camera Calibration by Viewing a Plane from Unknown Orientations. International Conference on Computer Vision (ICCV'99): 666-673.

[15] Trucco, E. & Verri, A. (1998). Introductory techniques for 3-D computer vision: Prentice-Hall.
[16] Sonka, M., Hlavac, V. & Boyle, R. (1995). Image Processing, Analysis and Machine Vision: Chapman and Hall.
[17] Forsyth, D. & Ponce, J. (2003). Computer Vision–A Modern Approach: Prentice Hall.
[18] WIT manual (2003). Version 7.2.1.
[19] Sun, W., Darling, A., Starly, B. & Nam, J. (2004). Computer-aided tissue engineering: overview, scope and challenges. Biotechnology and Applied Biochemistry; Vol 39: 29-47.
[20] Hohne, K. H. (2002). Medical image computing at the Institute of Mathematics and Computer Science in Medicine, University Hospital Hamburg-Eppendorf. IEEE Transactions on Medical Imaging; Vol 21: 713–723.
[21] Ausiello, P., Rengo, S., Davidson, C.L. & Watts, D.C. (2004). Stress Distributions in adhesively cemented ceramic and resin-composite Class II inlay restorations: a 3D-FEA study. Dental Materials; Vol 20: 862-872.
[22] Ausiello, P., Apicella, A., Davidson, C.L. & Rengo, S. (2001). 3D-finite element analyses of cusp movements in a human upper premolar, restored with adhesive resin-based composites. Journal of Biomechanics; Vol 24: 1269-1277.
[23] Three-Dimensional Tooth Profiling System for Evaluating Dental Materials Wear. http://www.mts.com/downloads/500005-86.pdf. MTS.
[24] Sakarya, U. & Erkmen, I. (2003). An improved method of photometric stereo using local shape from shading. Image and Vision Computing: Vol. 21; 941-954.
[25] Imageware (2003). Imageware Course guide: Modelling I, MDA 190-11. UGS.
[26] Klette, R., Schlüns, K. & Koschan, A. (1998). Computer Vision: 3-D Data From Images: Springer.
[27] Vision Elements, 'The Machine Vision Handbook' (2004/2005). First Sight Vision. http://www.firstsightvision.co.uk.
[28] Galantucci, L.M., Percoco, G. & Spina, R (2004). An artificial intelligence approach to registration of free-form shapes. CIRP Annals: 139-142.
[29] Burgess, S.C., Alemzadeh, K. & Zhang, L. (2004). The development of a miniature mechanism for producing insect wing motion. Design and Nature; Vol 6: 237-244.